

$(\eta^3\text{-Azaallyl})\text{zirconium Chlorides: Synthesis, Characterization, and Ethylene (Co-)polymerization Activity}$

Shifang Yuan,^{†,‡} Shengdi Bai,[†] Diansheng Liu,^{*,†} and Wen-Hua Sun^{*,‡}

[†]*Institute of Applied Chemistry, Shanxi University, Taiyuan 030006, People's Republic of China, and*
[‡]*Key Laboratory of Engineering Plastics and Beijing National Laboratory for Molecular Sciences, Institute of Chemistry, Chinese Academy of Sciences, Beijing 100190, People's Republic of China*

Received February 21, 2010

(2,6-Diisopropyl-*N*-(1-phenylvinyl)benzenamido)magnesium bromide ($\text{CH}_2(\text{Ph})\text{C}(2,6\text{-}i\text{Pr}_2\text{C}_6\text{H}_3)\text{-NMgBr}\cdot 2\text{THF}$, **1b**) reacted with 1 equiv of $\text{Me}_2\text{NMe}_2\text{SiCl}$ to form the *N*-(2-((dimethylamino)dimethylsilyl)-1-phenylvinyl)-2,6-diisopropylbenzenamine (**1c**). The stoichiometric reaction of **1c** with lithium diisopropylamide (LDA) formed lithium *N*-(2-((dimethylamino)dimethylsilyl)-1-phenylvinyl)-2,6-diisopropylbenzenamidate ($\text{Me}_2\text{NMe}_2\text{SiCH}(\text{Ph})\text{C}(2,6\text{-}i\text{Pr}_2\text{C}_6\text{H}_3)\text{NLi}\cdot 3\text{THF}$, **1d**) in high yields. The reaction of zirconium tetrachloride with 2 equiv of **1d** produced the bisligated $(\eta^3\text{-azaallyl})\text{zirconium dichloride}$ ($(\eta^3\text{-}(2,6\text{-}i\text{Pr}_2\text{C}_6\text{H}_3)\text{N}(\text{Ph})\text{CCHSiMe}_2\text{NMe}_2)_2\text{ZrCl}_2$, **2**), whereas the stoichiometric reaction of zirconium tetrachloride with **1d** formed a monoligated zirconium trichloride complex ($(\eta^3\text{-}\eta^1\text{-}(2,6\text{-}i\text{Pr}_2\text{C}_6\text{H}_3)\text{N}(\text{Ph})\text{CCHSiMe}_2\text{NMe}_2)\text{ZrCl}_3$, **3**), in which the ligand acted as an $\eta^3\text{-azaallyl}$ species with N-donation via the dimethylamino group at the silyl bridge. All compounds were fully characterized by elemental and spectroscopic analyses and metal compounds by single-crystal X-ray diffraction. The azaallyl groups of the ligands act in a $\kappa^1\text{-enamido}$ fashion in compounds **1b,d**, while the azaallyls appear as an $\eta^3\text{-}N,C,C$ mode in compound **2**. The $\eta^3\text{:}\eta^1$ coordination of the azaallyl and dimethylsilyl groups provided a sterically constrained geometry around the zirconium in compound **3**. The coordination geometries around each zirconium are pseudo-octahedral in both compounds **2** and **3**. The modes of coordination affected their catalytic behaviors toward polymerization: high activity by **3** and good activity by **2**.

1. Introduction

(Azaallyl)metal complexes have drawn much attention due to the diverse bonding modes of azaallyl groups such as the terminal $\kappa^1\text{-enamido}$ (I) and a monometallic (II) and

bimetallic η^3 fashion (III) (Scheme 1).¹ Numerous complexes of the main-group elements^{1–3} and transition metals^{4–7} have been explored. Our efforts have focused on the $(\eta^3\text{-azaallyl})\text{zirconium complexes}$ ⁴ because of the great potential of zirconium complexes in producing polyolefins with unique properties.⁸ The zirconium procatalysts⁹ are mainly divided as metallocene derivatives¹⁰ and half-metallocene derivatives.¹¹ In fact, the bridged $\eta^5\text{:}\eta^1$ -coordinated half-metallocenes, namely constrained geometry compounds (CGC), have been extensively investigated,¹¹ and an analogous

*To whom correspondence should be addressed. Tel: +86-10-62557955. Fax: +86-10-62618239. E-mail: dsliu@sxu.edu.cn (D.-S.L.); whsun@iccas.ac.cn (W.-H.S.).

(1) (a) Caro, C. F.; Lappert, M. F.; Merle, P. G. *Coord. Chem. Rev.* **2001**, 219–221, 605. (b) Hitchcock, P. B.; Lappert, M. F.; Liu, D.-S. *J. Chem. Soc., Chem. Commun.* **1994**, 2637. (c) Hitchcock, P. B.; Lappert, M. F.; Layh, M.; Liu, D.-S.; Sablong, R.; Shun, T. *Dalton Trans.* **2000**, 2301.

(2) (a) Hitchcock, P. B.; Lappert, M. F.; Sablong, R. *Dalton Trans.* **2006**, 4146. (b) Merle, L. B.; Hitchcock, P. B.; Lappert, M. F.; Merle, P. G. *Dalton Trans.* **2008**, 3493. (c) Shaviv, E.; Botoshansky, M.; Eisen, M. S. *J. Organomet. Chem.* **2003**, 683, 165. (d) Nelkenbaum, E.; Kapon, M.; Eisen, M. S. *J. Organomet. Chem.* **2005**, 690, 2297. (e) Fernandes, M. A.; Layh, M.; Omondi, B. *Polyhedron* **2005**, 24, 958.

(3) (a) Hitchcock, P. B.; Liu, D.-S. *J. Organomet. Chem.* **2003**, 683, 83. (b) Chen, X.; Guan, L.; Eisen, M. S.; Li, H.; Tong, H.; Zhang, L.; Liu, D.-S. *Eur. J. Inorg. Chem.* **2009**, 3488.

(4) (a) Lappert, M. F.; Liu, D.-S. *J. Organomet. Chem.* **1995**, 500, 203. (b) Lappert, F. Liu, D.-S. *Neth. Pat. Appl.* 9500085, **1995**. (c) Lappert, M. F.; Liu, D.-S. *Neth. Pat. Appl.* 9400919, **1994**. (d) Lappert, M. F.; Raston, C. L.; Skelton, B. W.; White, A. H. *J. Chem. Soc., Chem. Commun.* **1982**, 14.

(5) (a) Hitchcock, P. B.; Hu, J.; Lappert, M. F. *Chem. Commun.* **1998**, 143. (b) Hitchcock, P. B.; Lappert, M. F.; Layh, M. *Z. Anorg. Allg. Chem.* **2000**, 626, 1081.

(6) (a) Bowen, R. J.; Fernandes, M. A.; Layh, M. *J. Organomet. Chem.* **2004**, 689, 1230. (b) Bowen, R. J.; Caddy, J.; Fernandes, M. A.; Layha, M.; Mamo, M. A. *Polyhedron* **2004**, 23, 2273.

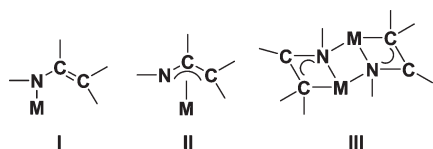
(7) (a) Leung, W. P.; So, C. W.; Chong, K. H.; Kan, K. W.; Chan, H. S.; Mak, T. C. W. *Organometallics* **2006**, 25, 2851. (b) Lorenz, V.; Görls, H.; Thiele, S. K.-H.; Scholz, J. *Organometallics* **2005**, 24, 797. (c) Avent, A. G.; Hitchcock, P. B.; Lappert, M. F.; Sablong, R.; Severn, J. R. *Organometallics* **2004**, 23, 2591.

(8) (a) Braunschweig, H.; Breitling, F. M. *Coord. Chem. Rev.* **2006**, 250, 2691. (b) Chum, P. S.; Kruper, W. J.; Guest, M. *J. Adv. Mater.* **2000**, 12, 1759.

(9) (a) Ziegler, K.; Gellert, H. G.; Zosel, K.; Lehmkuhl, W.; Pfohl, W. *Angew. Chem.* **1955**, 67, 424. (b) Ziegler, K.; Holzkamp, E.; Breil, H.; Martin, H. *Angew. Chem.* **1955**, 67, 541. (c) Natta, G. *J. Polym. Sci.* **1955**, 16, 143. (d) Natta, G.; Pino, P.; Corradini, P.; Danusso, F.; Mantica, E.; Mazzanti, G.; Moraglio, G. *J. Am. Chem. Soc.* **1955**, 77, 1708. (e) Groppo, E.; Lamberti, C.; Bordiga, S.; Spoto, G.; Zecchina, A. *Chem. Rev.* **2005**, 105, 115.

(10) (a) Sinn, H.; Kaminsky, W.; Vollmer, H.-J.; Woldt, R. *Angew. Chem., Int. Ed. Engl.* **1980**, 19, 390. (b) Kaminsky, W. *Macromol. Chem. Phys.* **1996**, 197, 3907. (c) Brintzinger, H. H.; Fischer, D.; Mühlaupt, R.; Rieger, B.; Waymouth, R. M. *Angew. Chem., Int. Ed. Engl.* **1995**, 34, 1143. (d) Alt, H. G.; Köppl, A. *Chem. Rev.* **2000**, 100, 1205.

Scheme 1. Bonding Modes of Azaallyl Groups

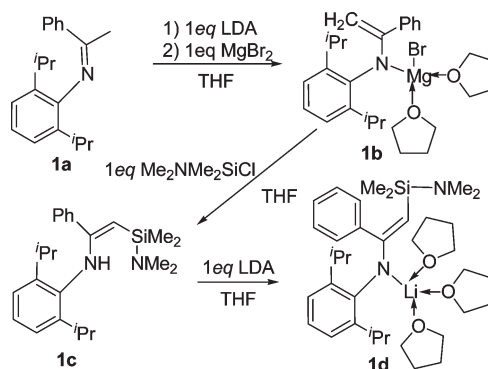
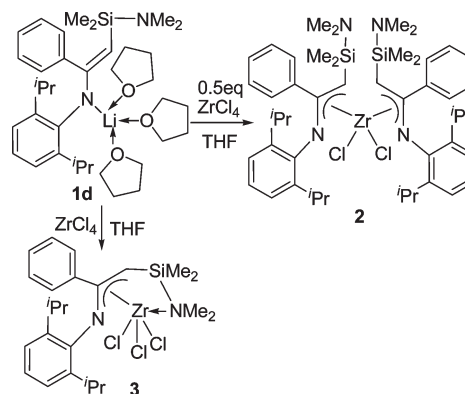


titanium catalyst has finally been commercialized.¹² In terms of the role of the η^5 ligand, the η^3 -azaallyl species can be considered as an alternative. In the model of the CGC, the bridged $\eta^5:\eta^1$ ligands have two negative charges; however, our efforts to obtain the bridged dianionic $\eta^3:\eta^1$ ligand were unsuccessful. Therefore, we have turned to the monoanionic bridged $\eta^3:\eta^1$ ligand in which the ligand contains an anionic η^3 function (η^3 -azaallyl) group and a neutral donating (amino) group. The monoanionic bridged $\eta^3:\eta^1$ coordination mode has been seen in metal allyls.¹³

In addition to the azaallylzirconium analogues,⁴ the 1-azaallylmetal complexes of magnesium ($\text{CH}_2(\text{Ph})\text{C}(2,6\text{-}i\text{Pr}_2\text{-C}_6\text{H}_3)\text{NMgBr}\cdot 2\text{THF}$, **1b**) and lithium ($\text{Me}_2\text{NMe}_2\text{SiCH}(\text{Ph})\text{C}(2,6\text{-}i\text{Pr}_2\text{-C}_6\text{H}_3)\text{NLi}\cdot 3\text{THF}$, **1d**) were successfully prepared. There is an extra dimethylamine bridge through the dimethylsilyl group on the azaallyl group in **1d**. When the molar ratio of **1d** to zirconium tetrachloride was controlled in each reaction, the bis(η^3 -azaallyl)zirconium dichloride ($(\eta^3\text{-}(2,6\text{-}i\text{Pr}_2\text{-C}_6\text{H}_3)\text{N}(\text{Ph})\text{CCHSiMe}_2\text{NMe}_2)_2\text{-ZrCl}_2$, **2**) and the silyl-bridged $\eta^3:\eta^1$ -coordinated zirconium trichloride ($(\eta^3:\eta^1\text{-}(2,6\text{-}i\text{Pr}_2\text{-C}_6\text{H}_3)\text{N}(\text{Ph})\text{-CCHSiMe}_2\text{NMe}_2)\text{ZrCl}_3$, **3**) were isolated. The procatalyst **2** revealed considerable catalytic activity toward ethylene polymerization; meanwhile, procatalyst **3** showed good activity in both ethylene polymerization and copolymerization of ethylene with 1-hexene. Herein the syntheses and characterization of all metal compounds are reported in detail as well as the catalytic behaviors of zirconium compounds in polymerization.

2. Results and Discussion

2.1. Synthesis and Characterization. The treatment of $\text{Me}(\text{Ph})\text{CN}(2,6\text{-}i\text{Pr}_2\text{-C}_6\text{H}_3)$ (**1a**) with 1 equiv of LDA (lithium diisopropylamide) and MgBr_2 in THF quantitatively produces the κ^1 -enamido magnesium complex $\text{CH}_2(\text{Ph})\text{C}(2,6\text{-}i\text{Pr}_2\text{-C}_6\text{H}_3)\text{NMgBr}\cdot 2\text{THF}$ (**1b**). The stoichiometric reaction of **1b** with $\text{Me}_2\text{NMe}_2\text{SiCl}$ in THF forms the compound $(2,6\text{-}i\text{Pr}_2\text{-C}_6\text{H}_3)\text{NC}(\text{Ph})\text{CH}_2\text{SiMe}_2\text{NMe}_2$ (**1c**). Subsequently the compound **1c** reacts with 1 equiv of LDA in THF to afford the κ^1 -enamido lithium compound $\text{Me}_2\text{NMe}_2\text{SiCH}(\text{Ph})\text{C}(2,6\text{-}i\text{Pr}_2\text{-C}_6\text{H}_3)\text{NLi}\cdot 3\text{THF}$ (**1d**). In addition to elemental and NMR analyses, the structures of **1b,d** were confirmed by single-crystal X-ray diffraction. The synthetic procedure is illustrated in Scheme 2.

Scheme 2. Syntheses of κ^1 -Enamido Metal CompoundsScheme 3. Synthesis of Zirconium Compounds **2** and **3**

The reaction of 2 equiv of **1d** with ZrCl_4 forms the bis(η^3 -azaallyl)zirconium dichloride ($\eta^3\text{-}(2,6\text{-}i\text{Pr}_2\text{-C}_6\text{H}_3)\text{N}(\text{Ph})\text{CCHSiMe}_2\text{NMe}_2)_2\text{ZrCl}_2$ (**2**) in good yields. Compound **2** is a colorless crystalline solid and is soluble in hydrocarbon solvents, similar to $\text{rac}\text{-}[\text{Zr}\{\text{N}(\text{SiMe}_3)\text{C}(\text{tBu})\text{C}(\text{SiMe}_3)_2\text{Cl}_2\}]_2$.⁴ The stoichiometric reaction of **1d** with ZrCl_4 , however, produced the monoligated zirconium trichloride complex ($\eta^3:\eta^1\text{-}(2,6\text{-}i\text{Pr}_2\text{-C}_6\text{H}_3)\text{N}(\text{Ph})\text{CCHSiMe}_2\text{NMe}_2\text{ZrCl}_3$ (**3**), in high yield (Scheme 3). In compound **3**, the ligand acts as a η^3 -azaallyl with an N-donor from the dimethylamine through the silyl bridge. This is the first example of bridged $\eta^3:\eta^1$ coordination in a zirconium trichloride. Compound **3** is soluble in THF and sparingly soluble in Et_2O and CH_2Cl_2 . The microanalysis and NMR spectra of all compounds are in agreement with their molecular structures, as confirmed by single-crystal X-ray diffraction.

2.2. Crystal Structures. The newly synthesized metal compounds are highly air and moisture sensitive. The molecular structure of the magnesium compound $\text{CH}_2(\text{Ph})\text{C}(2,6\text{-}i\text{Pr}_2\text{-C}_6\text{H}_3)\text{NMgBr}\cdot 2\text{THF}$ (**1b**) is shown in Figure 1 with selected bond lengths and angles given in the caption. The magnesium atom of compound **1b** is four-coordinate with a typical terminal κ^1 -enamido (**I**, Scheme 1), a bromide, and two oxo donors of tetrahydrofuran (thf) molecules. This is a common feature wherein additional “solvent” molecules act as neutral donors, and this coordination can stabilize the complexes.¹ The Mg-N distance ($\text{Mg-N} = 1.995(5)$ Å) is slightly shorter than the previously reported distance ($\text{Mg-N} = 2.015(2)$ Å).¹⁴ $\text{C}(1)\text{-N}$ ($1.373(7)$ Å) is slightly shorter than $\text{C}(9)\text{-N}$ ($1.449(7)$ Å), due to the “charge” delocalization

(11) (a) McKnight, A. L.; Waymouth, R. M. *Chem. Rev.* **1998**, *98*, 2587. (b) Britovsek, G. J. P.; Gibson, V. C.; Wass, D. F. *Angew. Chem.* **1999**, *111*, 448. (c) Britovsek, G. J. P.; Gibson, V. C.; Wass, D. F. *Angew. Chem., Int. Ed. Engl.* **1999**, *38*, 428. (d) Imanishi, Y.; Naga, N. *Prog. Polym. Sci.* **2001**, *26*, 1147. (e) Arndt, S.; Okuda, J. *Chem. Rev.* **2002**, *102*, 1953. (f) Okuda, J. *Dalton Trans.* **2003**, 2367. (g) Gibson, V. C.; Spitzmesser, S. K. *Chem. Rev.* **2003**, *103*, 283. (h) Qian, Y.; Huang, J.; Bala, M. D.; Lian, B.; Zhang, H. *Chem. Rev.* **2003**, *103*, 2633.

(12) (a) Stevens, J. C.; Timmers, F. J.; Wilson, D. R.; Schmidt, G. F.; Nickias, P. N.; Rosen, R. K.; McKnight, G. W.; Lai, S. *Eur. Pat. Appl.* 0416815A2, **1991**. (b) Shapiro, P. J.; Bunel, E.; Schaefer, W. P.; Bercaw, J. E. *Organometallics* **1990**, *9*, 867. (c) Shapiro, P. J.; Cotter, W. D.; Schaefer, W. P.; Labinger, J. A.; Bercaw, J. E. *J. Am. Chem. Soc.* **1994**, *116*, 4623.

(13) (a) Solomon, S. A.; Layfield, R. A. *Dalton Trans.* **2010**, *39*, 2469. (b) Solomon, S. A.; Muryn, C. A.; Layfield, R. A. *Chem. Commun.* **2008**, 3142. (c) Strohmman, C.; Lehmen, K.; Dilsky, S. *J. Am. Chem. Soc.* **2006**, *128*, 8102.

(14) Fedushkin, I. L.; Makarov, V. M.; Rosenthal, E. C. E.; Fukin, G. K. *Eur. J. Inorg. Chem.* **2006**, 827.

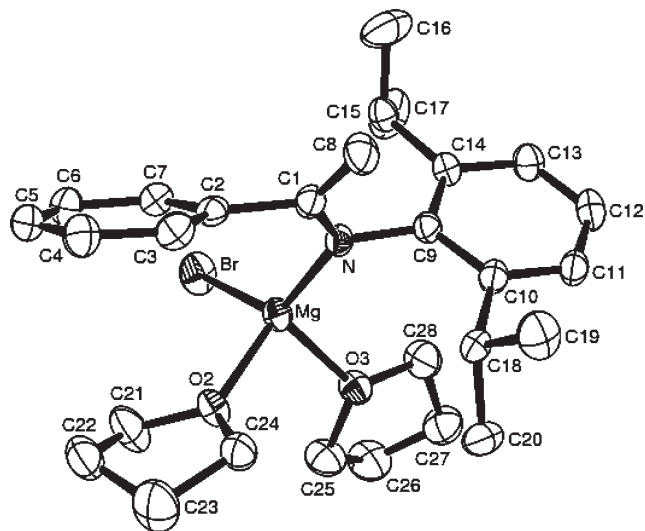


Figure 1. Molecular structure of compound **1b** with all hydrogen atoms omitted for clarity. Thermal ellipsoids are shown at the 30% probability level. Selected bond lengths (Å) and bond angles (deg): Mg–N = 1.995(5), Mg–O(2) = 2.018(4), Mg–O(3) = 2.029(5), Mg–Br = 2.457(2), N–C(1) = 1.373(7), N–C(9) = 1.449(7), C(1)–C(8) = 1.365(9), C(1)–C(2) = 1.502(8); N–Mg–Br = 127.76(16), C(1)–N–C(9) = 115.0(4), C(8)–C(1)–N = 126.9(5), C(8)–C(1)–C(2) = 117.7(5), N–C(1)–C(2) = 115.4(5), C(9)–N–Mg = 116.6(3), C(1)–N–Mg = 128.3(4), O(2)–Mg–O(3) = 95.55(19).

from the double bond C(1)–C(8) (= 1.365(9) Å). The dihedral angle of C(2)–C(1)–C(8) and C(9)–N–Mg is 7.16°, and that of the planes C(8)–C(1)–N and C(1)–N–Mg is 9.09°, which might be partially due to the steric repulsion between the rotation of two large phenyl groups. The dihedral angles of two phenyl rings with the plane C(8)–C(1)–N–Mg are 79.03 and 45.45°, respectively.

The molecular structure of the terminal κ^1 -enamido lithium compound $\text{Me}_2\text{NMe}_2\text{SiCH}(\text{Ph})\text{C}(\text{C}_2,6\text{-}^i\text{Pr}_2\text{C}_6\text{H}_3)\text{-NLi}\cdot 3\text{THF}$ (**1d**) is shown in Figure 2, with selected bond lengths and angles given in the caption. (η^3 -Azaallyl)lithium compounds have previously been studied, and some comparable compounds are $[\text{LiN}(\text{Ar})\text{C}(\text{R})\text{CHR}(\text{thf})_2]_2^{\text{c}}$, $[\text{LiN}(\text{R})\text{-C}(\text{Ar})\text{CR}_2(\text{thf})]_2^{\text{c}}$, $[\text{LiN}(\text{Ar})\text{C}(\text{H})\text{CH}^n\text{Pr}(\text{thf})_3]_2^{\text{c}}$, and (with a neutral coordinating dimethylamide group) $[\text{LiN}(\text{SiMe}_2\text{-NMe}_2)\text{C}(\text{tBu})\text{CHPh}(\text{tmeda})]_2^{\text{c}}$.¹⁷ As a result of steric crowding, the lithium compound **1d** is uniquely a Z isomer with wider angles around the sp^2 -hybridized carbons C(13) and C(20): N(1)–C(13)–C(20) = 127.8(3)°, C(13)–C(20)–Si = 131.8(3)°, C(20)–Si–N(2) = 115.1(2)°. The five atoms Li, N(1), C(13), C(20), and Si are almost coplanar, with the largest deviation from planarity being 0.018(1) Å for C(20), while the distance between the plane and N(2) is 1.157 Å. In addition, the plane of Li, N(1), C(13), C(20), and Si is approximately perpendicular to the two phenyl rings with dihedral angles of 89.59 and 72°.

The molecular structure of the crystalline compound (η^3 -(2,6- $^i\text{Pr}_2\text{C}_6\text{H}_3$)N(Ph)CCHSiMe₂NMe₂)₂ZrCl₂ (**2**) is illustrated in Figure 3, with selected bond lengths and angles

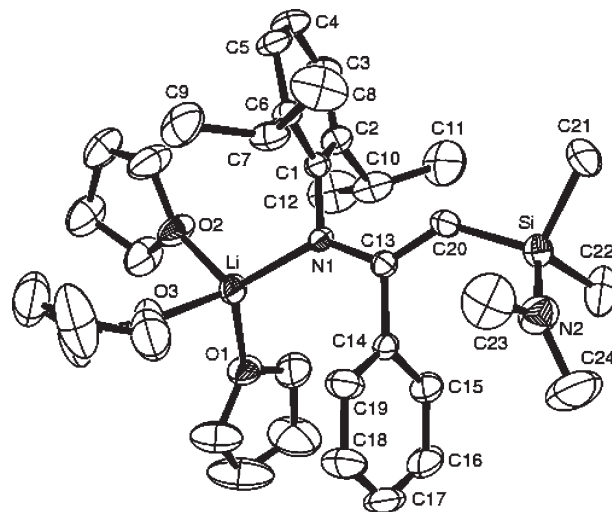


Figure 2. Molecular structure of compound **1d** with all hydrogen atoms omitted for clarity. Thermal ellipsoids are shown at the 30% probability level. Selected bond lengths (Å) and bond angles (deg): Li–N(1) = 2.011(7), Li–O(1) = 1.983(7), Li–O(2) = 2.041(7), Li–O(3) = 2.021(8), N(1)–C(13) = 1.352(4), N(1)–C(1) = 1.408(4), N(2)–C(24) = 1.419(7), N(2)–C(23) = 1.445(7), C(13)–C(20) = 1.372(5), N(2)–Si = 1.703(4), C(13)–C(14) = 1.509(5), Si–C(20) = 1.829(4), Si–C(22) = 1.875(5), Si–C(21) = 1.884(5); N(1)–C(13)–C(20) = 127.8(3), N(2)–Si–C(20) = 115.1(2), C(13)–N(1)–Li = 132.6(3), C(13)–C(20)–Si = 131.8(3), C(1)–N(1)–Li = 111.2(3), C(13)–N(1)–C(1) = 116.0(3), C(20)–C(13)–C(14) = 119.0(3), O(1)–Li–O(2) = 97.5(3), O(2)–Li–O(3) = 97.0(3), O(1)–Li–O(3) = 101.6(3).

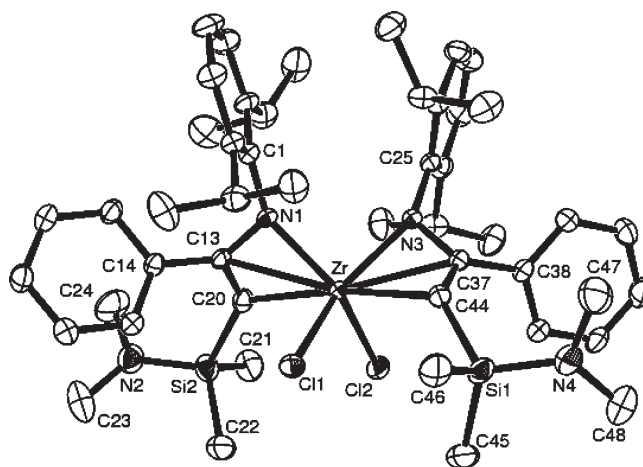


Figure 3. Molecular structure of compound **2**, with all hydrogen atoms omitted for clarity. Thermal ellipsoids are shown at the 30% probability level. Selected bond lengths (Å) and bond angles (deg): Zr–N(1) = 2.101(4), Zr–N(3) = 2.107(4), Zr–C(20) = 2.593(5), Zr–C(44) = 2.570(5), Zr–Cl(2) = 2.4242(15), Zr–Cl(1) = 2.4233(15), N(3)–C(37) = 1.394(6), N(1)–C(13) = 1.392(7), N(3)–C(25) = 1.460(6), N(1)–C(1) = 1.462(6), Si(2)–C(20) = 1.854(6), Si(1)–C(44) = 1.885(5), N(4)–Si(1) = 1.690(6), N(2)–Si(2) = 1.684(6), C(13)–C(14) = 1.493(7), C(13)–C(20) = 1.409(8), C(37)–C(44) = 1.355(7), C(37)–C(38) = 1.499(7); N(1)–Zr–N(3) = 89.84(16), Cl(2)–Zr–Cl(1) = 99.31(6), N(1)–Zr–C(44) = 126.33(17), N(3)–Zr–C(44) = 58.63(16), N(1)–Zr–C(20) = 59.52(17), N(3)–Zr–C(20) = 128.43(17), C(13)–N(1)–C(1) = 120.6(4), C(37)–N(3)–Zr = 92.7(3), C(13)–N(1)–Zr = 93.7(3), N(4)–Si(1)–C(44) = 111.1(3), C(1)–N(1)–Zr = 141.5(3), N(2)–Si(2)–C(20) = 111.3(3).

(15) Lappert, M. F.; Layh, M. *Tetrahedron Lett.* **1998**, 39, 4745.

(16) Bosold, F.; Marsch, M.; Harms, K.; Boche, G. *Z. Kristallogr.-New Cryst. Struct.* **2001**, 216, 427.

(17) Shi, H. P.; Liu, D.-S.; Huang, S.-P. *Acta Crystallogr., Sect. E* **2003**, 59, m339.

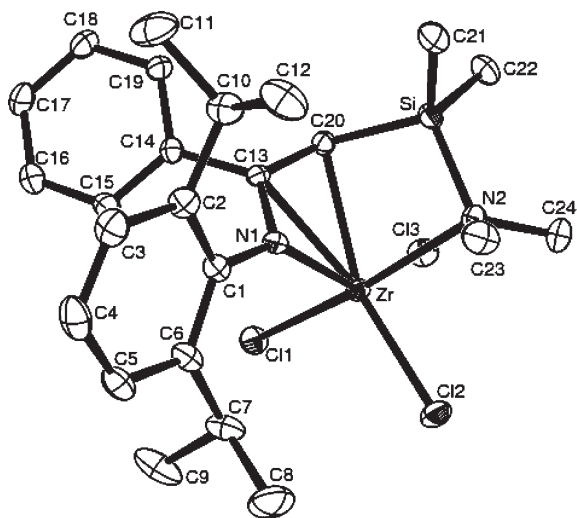


Figure 4. Molecular structure of compound **3**, with all hydrogen atoms omitted for clarity. Thermal ellipsoids are shown at the 30% probability level. Selected bond lengths (Å) and bond angles (deg): Zr–N(1) = 2.179(3), Zr–N(2) = 2.406(4), Zr–C(20) = 2.467(4), Zr–Cl(1) = 2.4172(15), Zr–Cl(2) = 2.3983(12), Zr–Cl(3) = 2.4172(12), N(1)–C(13) = 1.378(5), N(1)–C(1) = 1.418(5), C(20)–C(13) = 1.371(6), C(14)–C(13) = 1.495(6), Si–C(20) = 1.868(5), Si–N(2) = 1.816(4); N(1)–Zr–N(2) = 87.83(13), N(2)–Zr–C(20) = 72.37(14), N(1)–Zr–C(20) = 59.99(12), N(2)–Si–C(20) = 102.69(18), C(13)–N(1)–C(1) = 121.1(3), C(13)–C(20)–Si = 128.0(3), C(13)–N(1)–Zr = 89.3(2), C(13)–C(20)–Zr = 78.1(2), Si–C(20)–Zr = 90.12(16), C(1)–N(1)–Zr = 143.6(3), Si–N(2)–Zr = 93.34(18), Cl(1)–Zr–Cl(2) = 101.99(5), Cl(2)–Zr–Cl(3) = 99.38(5), Cl(1)–Zr–Cl(3) = 87.21(4).

given in the caption. The central zirconium is coordinated with two chlorides and two anionic η^3 -azaallyl ligands in a cis mode. The two zirconacycles Zr–N–C–C are not symmetric. The dihedral angle between the planes N(1)–Zr–C(20) and N(3)–Zr–C(44) is 59.71°, while the angle between N(1)–Zr–C(20) and N(1)–C(13)–C(20) is 47.03°, and as a consequence the atom C(13) is out of the C(20)–Zr–N(1) plane (mean deviation 0.547 Å). The dihedral angle of 28.01° between N(1)–C(13)–C(20) and C(20)–Si–N(2) is smaller than that of 45.23° in **1d**. The bond distances Zr–N = 2.10 Å and Zr–C = 2.58 Å and bond angles N–Zr–C = 58.6° and N–C–C = 115.5° are similar to the data for Zr{N(R)C-(*t*Bu)CH₂C₆H₄-2}Cl₂,⁴ in which a bridged η^3 -azaallyl ligand was observed.

The molecular structure of the compound (η^3 : η^1 -(2,6-*i*Pr₂C₆H₃)N(Ph)CCHSiMe₂NMe₂)ZrCl₃ (**3**) is illustrated in Figure 4, with selected bond lengths and angles given in the caption. As shown in the figure, the zirconium is bonded to three chlorides and one bridged ligand acting as an anionic η^3 -azaallyl with the pendant arm coordinated via N(CH₃)₂. In the N–C–C–Si–N moiety, the bond angles N(1)–C(13)–C(20), C(13)–C(20)–Si, and Si–C(20)–N(2) are 116.4(4), 128.0(13), and 102.69(18)°, respectively. N(1)–C(13)–C(20) exists in the η^3 -azaallyl form as a conjugated system with N(1)–C(13) = 1.378(5) Å and C(20)–C(13) = 1.371(6) Å. The Zr–N(1) bond distance in **3** is slightly longer than that in a similar compound,⁴ while the Zr–C bond distances are shorter than those of that similar compound.⁴ The dihedral angle between C(20)–C(13)–N(1) and C(20)–Zr–N(1) is 46.47°, and the distance of the atom

Table 1. Ethylene Polymerization of the Compound **2**/MAO^a

entry	<i>P</i> (atm)	<i>T</i> (°C)	Al/Zr	activity ^b	<i>T</i> _m (°C) ^c	<i>M</i> _w ^d	<i>M</i> _w / <i>M</i> _n ^d
1	1	30	1000	trace			
2	1	50	1000	2.10	134.4		
3	1	70	1000	trace			
4	10	30	500	3.94	135.8	8.20	4.2
5	10	30	1000	4.64	134.9	7.90	14
6	10	30	1500	3.72	134.1	5.76	29
7	10	50	1000	6.47	133.6	5.19	8.2
8	10	60	1000	6.89	133.3	3.05	7.7
9	10	70	1000	8.12	133.1	4.77	7.0
10	10	80	1000	6.34	132.4	2.27	4.4

^a Conditions: catalyst, 5 μmol; time, 30 min; total volume, 30 mL of toluene for 1 atm or 100 mL of toluene for 10 atm. ^b In units of 10⁴ g (mol of Zr)⁻¹ h⁻¹ atm⁻¹. ^c Determined by DSC. ^d In units of 10⁵ g mol⁻¹; determined by GPC.

C(13) from C(20)–Zr–N(1) plane is 0.525 Å. The dihedral angle between C(20)–Si–N(2) and C(20)–Zr–N(2) is 13°; hence, the atom Si is out of the C(20)–Zr–N(2) plane (mean deviation 0.259 Å). The dihedral angle of C(20)–Zr–N(1) and C(20)–Zr–N(2) is approximately perpendicular at 82.09°. The dihedral angles of phenyl rings to the η^3 -azaallyl N(1)–C(13)–C(20) plane are 64.52 and 35.69°. The η^3 : η^1 -(2,6-*i*Pr₂C₆H₃)N(Ph)CCHSiMe₂NMe₂ ligand provides a constrained geometry around zirconium, which can be considered as an alternative species for the CGC catalysts.¹²

2.3. Ethylene Polymerization. Ethylene polymerization using procatalyst **2** was investigated in the presence of MAO (Table 1). Good activities were obtained when the [Al]/[Zr] molar ratio was increased from 500 to 1000; however, a further increase to 1500 led to a decrease of catalytic activity (entries 4–6 in Table 1). Probably the active species was suppressed by an excess of MAO, as suggested in the literature;¹⁸ moreover, the amount of AlMe₃ contained in MAO led to deactivation. At an Al/Zr molar ratio of 1000 at 1 atm of ethylene, the highest activity was obtained, 2.10 × 10⁴ g (mol of Zr)⁻¹ h⁻¹ atm⁻¹, at a reaction temperature of 50 °C. Increasing the ethylene pressure from 1 to 10 atm led to a further increase in polymerization activity to 8.12 × 10⁴ g (mol of Zr)⁻¹ h⁻¹ atm⁻¹ at 70 °C (entry 9 in Table 1). At low reaction temperature (30 °C), the polymers show high molecular weights but broad molecular weight distributions, which is consistent with the literature.¹⁹

Ethylene polymerization using procatalyst **3** was also investigated (Table 2). Alkylaluminums such as AlEt₃ and Et₂AlCl do not activate zirconium compound **3** for ethylene polymerization over a range of concentrations and reaction temperatures (entries 1 and 2 in Table 2). However, moderate activities are observed with both MMAO (entry 3 in Table 2) and MAO (entry 4 in Table 2). Accordingly, MAO was selected as a practical activator for further investigations. Using Al/Zr molar ratios in the range 500–1500 (entries 5–7 in Table 2) at 1 atm ethylene pressure and 50 °C, the maximum activity was obtained at an Al/Zr molar ratio of 1000 (entry 5 in Table 2). With reaction temperatures in the range 30–70 °C at 1 atm of ethylene pressure with an Al/Zr molar ratio of 1000, the catalytic activity showed a maximum

(18) Chen, E.-Y.; Marks, T. J. *Chem. Rev.* **2000**, *100*, 1391.

(19) (a) Vollmerhaus, R.; Rahim, M.; Tomaszewski, R.; Xin, S.; Taylor, N. J.; Collins, S. *Organometallics* **2000**, *19*, 2161. (b) Xie, G.; Qian, C. J. *Polym. Sci., A: Polym. Chem.* **2008**, *46*, 211. (c) Kim, W. K.; Fevola, M. J.; Liable-Sands, L. M.; Rheingold, A. L.; Theopold, K. H. *Organometallics* **1998**, *17*, 4541.

Table 2. Ethylene Polymerization of the Compound 3^a

entry	cocat.	<i>P</i> (atm)	<i>T</i> (°C)	Al/Zr	acti- vity ^b	<i>T</i> _m (°C) ^c	<i>M</i> _w ^d	<i>M</i> _w / <i>M</i> _n ^d
1	Et ₂ AlCl	1	30	200	trace			
2	AlEt ₃	1	30	200	trace			
3	MMAO	1	30	1000	0.12	135.3		
4	MAO	1	30	1000	0.54	134.4		
5	MAO	1	50	500	0.93	133.9		
6	MAO	1	50	1000	1.35	132.6	3.23	41
7	MAO	1	50	1500	1.05	132.2		
8	MAO	1	70	1000	0.65	132.1		
9	MAO	10	30	500	0.41	136.4	6.20	6.6
10	MAO	10	30	1000	0.86	136.1	4.49	11
11	MAO	10	30	1500	0.46	133.8	3.86	20
12	MAO	10	50	1000	2.58	134.0	19.7	9.4
13	MAO	10	60	1000	2.96	133.9	65.8	6.7
14	MAO	10	70	1000	3.65	133.6	34.5	6.0
15	MAO	10	80	1000	1.72	133.5	27.8	3.8

^a Conditions: catalyst, 5 μmol; time, 30 min; cocatalyst, MAO; total volume, 30 mL of toluene for 1 atm or 100 mL of toluene for 10 atm. ^b In units of 10⁵ g (mol of Zr)⁻¹ h⁻¹ atm⁻¹. ^c Determined by DSC. ^d In units of 10⁵ g mol⁻¹; determined by GPC.

value of 1.35 × 10⁵ g (mol of Zr)⁻¹ h⁻¹ atm⁻¹ at 50 °C (entry 6 in Table 2), and the resultant polyethylene showed a *M*_w value of 3.23 × 10⁵ g mol⁻¹. As shown by DSC analysis, the resultant polyethylenes have only one melting point, indicating the monodisperse nature of the polymers. The melting points decreased slightly with increasing reaction temperatures (entries 4, 6, and 8 in Table 2) or the Al/Zr molar ratio (entries 5–7 in Table 2). The PEs obtained at low ethylene pressure showed broader molecular weight distributions.

With the ethylene pressure increased, the catalytic activity generally improved and gave higher molecular weights.^{20,21} In the current system, the activity is greatly affected by the ethylene pressure (cf. Table 2, entries 6 and 14). The polyethylene obtained possessed melting temperatures in the range of 132–136 °C, typical for high-density polyethylene (HDPE). Higher reaction temperatures led to narrower molecular distributions, whereas increasing the Al/Zr molar ratio led to broader molecular weight distributions. The broad MWD indicated the existence of multiple active species; such phenomena were observed in our previous work.^{19,22}

2.4. Ethylene/1-Hexene Copolymerization. The results of the copolymerization of ethylene/1-hexene by 2/MAO are illustrated in Table 3. The ethylene pressure was 10 atm, while the amount of 1-hexene was varied (entries 1–3 in Table 3). There is a positive comonomer effect; higher activities were generally observed in copolymerization (Table 3) than in the homopolymerization of ethylene (Table 1). As was the case in ethylene polymerizations, the optimum reaction temperature was 70 °C, with the highest activity for copolymerization at ~9 × 10⁴ g (mol of Zr)⁻¹ h⁻¹ atm⁻¹ (entry 6 in Table 3). When the 1-hexene concentration and reaction temperature were increased, the *T*_m and *M*_w values for the obtained copolymers gradually decreased; however, the MWD values increased with the concentration of 1-hexene but decreased with elevating reaction temperature.

(20) Yang, X.; Zhang, Y.; Huang, J. *J. Mol. Catal., A: Chem.* **2006**, *250*, 145.

(21) Suzuki, N.; Masubuchi, Y.; Yamaguchi, Y.; Kase, T.; Miyamoto, T.; Horiuchi, A.; Mise, T. *Macromolecules* **2000**, *33*, 754.

(22) (a) Zuo, W. W.; Zhang, M.; Sun, W.-H. *J. Polym. Sci., Part A: Polym. Chem.* **2009**, *47*, 357. (b) Hong, H.; Zhang, Z.; Chung, T. C.; Lee, R. W. *J. Polym. Sci., Part A: Polym. Chem.* **2007**, *45*, 639. (c) Smit, M.; Zheng, X.; Loos, J.; Chadwick, J. C.; Koning, C. E. *J. Polym. Sci., Part A: Polym. Chem.* **2006**, *44*, 6652.

Table 3. Ethylene and 1-Hexene Copolymerization of the Compound 2/MAO^a

entry	<i>T</i> (°C)	amt of 1-hexene (mL)	acti- vity ^b	<i>T</i> _m (°C) ^c	<i>M</i> _w ^d	<i>M</i> _w / <i>M</i> _n ^d
1	30	4	4.24	133.1	19.3	18
2	30	6	5.68	132.7	23.6	24
3	30	8	4.08	131.3	11.5	36
4	50	6	6.24	129.1	4.49	11
5	60	6	7.76	127.9	3.86	11
6	70	6	8.96	127.4	3.03	8.4
7	80	6	6.48	126.8	1.90	6.3

^a Conditions: catalyst, 5 μmol; time, 30 min; cocatalyst, MAO; Al/Zr, 1000; total volume, 100 mL of toluene for 10 atm. ^b In units of 10⁴ g (mol of Zr)⁻¹ h⁻¹ atm⁻¹. ^c Determined by DSC. ^d In units of 10⁵ g mol⁻¹; determined by GPC.

Table 4. Ethylene and 1-Hexene Copolymerization of the Compound 3/MAO^a

entry	<i>P</i> (atm)	<i>T</i> (°C)	Al/Zr	amt of 1-hexene (mL)	acti- vity ^b	<i>T</i> _m (°C) ^c	<i>M</i> _w ^d	<i>M</i> _w / <i>M</i> _n ^d
1	1	50	1000	6	0.24	126.6		
2	10	30	500	6	0.72	132.3	3.40	7.6
3	10	30	1000	5	0.65	130.9	2.87	5.6
4	10	30	1000	6	0.89	132.0	4.85	11
5	10	30	1000	7	0.59	132.8	4.28	13
6	10	30	1500	6	0.54	131.9	6.15	36
7	10	50	1000	6	1.72	129.2	15.4	11
8	10	60	1000	6	2.86	128.5	16.8	10
9	10	70	1000	6	3.25	127.4	27.7	7.6
10	10	80	1000	6	1.68	126.6	8.82	6.4

^a Conditions: catalyst, 5.0 μmol; time, 30 min; cocatalyst, MAO; total volume, 30 mL of toluene for 1 atm or 100 mL of toluene for 10 atm. ^b In units of 10⁵ g (mol of Zr)⁻¹ h⁻¹ atm⁻¹. ^c Determined by DSC. ^d In units of 10⁵ g mol⁻¹; determined by GPC.

Similar trends of relationship of catalytic activity for the 3/MAO system and the nature of the resultant polymers were observed on varying the reaction parameters, and the results are tabulated in Table 4. The important feature of procatalyst 3 is its higher catalytic activity and better incorporation of 1-hexene, which is confirmed by the lower melting points (126–133 °C) compared with that of linear polyethylene. High activities were maintained at elevated temperature (entries 7–10, Table 4), a feature which is relevant to industrial operation. The resultant polymers, however, showed broader MWD values; the *M*_w values for the copolymers indicated suitable for the applicable consideration.

¹³C NMR analysis of the resultant poly(ethylene-co-1-hexene) revealed a typical ¹³C NMR spectrum of linear low-density polyethylene (LLDPE).²³ The 1-hexene incorporation reached 1.92 mol % using 2/MAO and 3.08 mol % using 3/MAO, and the representative ¹³C NMR spectra are shown in the Supporting Information.

Procatalysts 2 and 3 both maintained their activities at reaction temperature in the range 50–80 °C. A significant difference in their catalytic performances was observed, with procatalyst 3 possessing an activity about one order higher than that observed for procatalyst 2. This behavior is

(23) (a) Yano, A.; Gasegawa, S.; Kaneko, T.; Sone, M.; Sato, M.; Akimoto, A. *Macromol. Chem. Phys.* **1999**, *200*, 1542–1553. (b) Quijada, R.; Galland, G. B.; Mauler, R. S.; de Menezes, S. C. *Macromol. Rapid Commun.* **1996**, *17*, 607. (c) Chu, K.-J.; Soares, J. B. P.; Penlidis, A. *Macromol. Chem. Phys.* **2000**, *201*, 340. (d) Zhang, Y.; Yang, X.; Yu, Y.; Qian, Y.; Huang, J. *Chin. J. Chem.* **2005**, *23*, 1081. (e) Czaja, K.; Bialek, M. *Polymer* **2001**, *42*, 2289.

thought to be due to structural differences in the procatalysts; procatalyst **3** contains a ligand acting as $\eta^3:\eta^1$ -(2,6- i -Pr₂C₆H₃)N(Ph)CCHSiMe₂NMe₂, reminiscent of constrained geometry.

3. Conclusion

The κ^1 -enamido azaallyl magnesium compound **1b** and lithium compound **1d** were synthesized, and the two zirconium compounds $\{\eta^3$ -(2,6- i -Pr₂C₆H₃)N(Ph)CCHSiMe₂NMe₂\}₂-ZrCl₂ (**2**) and $\{\eta^3:\eta^1$ -(2,6- i -Pr₂C₆H₃)N(Ph)CCHSiMe₂NMe₂\}-ZrCl₃ (**3**) were prepared by employing the same ligand, but acting in different coordination modes. All metal compounds were structurally characterized by single-crystal X-ray diffraction. Procatalysts **2** and **3** were both screened for ethylene polymerization and copolymerization of ethylene with 1-hexene, producing polymers with high molecular weights and broad molecular distributions. These resultant polymers showed broader GPC curves, and only one T_m value for every polymer sample was observed. The procatalyst **3** showed 1 order higher activity than did the procatalyst **2**, thought to be due to the bridged ligand at zirconium forming a constrained-geometry type catalyst. Work on constrained-geometry compounds (CGC) has previously focused on the bridged dianionic $\eta^5:\eta^1$ ligands and their IVB metal complexes,¹² whereas the current result has explored the bridged monoanionic $\eta^3:\eta^1$ -ligands and their IVB metal complexes.

4. Experimental Section

4.1. General Procedures. All manipulations were carried out under an atmosphere of argon using standard Schlenk techniques. Solvents were purchased from commercial sources. The deuterated solvents C₆D₆ and CDCl₃ were dried over activated molecular sieves (4 Å) and vacuum-transferred before use. Hexane was dried using sodium potassium alloy. Diethyl ether was dried and distilled from sodium/benzophenone and stored over a sodium mirror under argon. Dichloromethane was distilled from activated molecular sieves (4 Å) or CaH₂. Toluene was refluxed in the presence of sodium/benzophenone and distilled under nitrogen prior to use. Glassware was oven-dried at 150 °C overnight. The NMR spectra were recorded on a Bruker DKX-300 spectrometer with TMS as the internal standard. Elemental analyses were performed with a Flash EA 1112 microanalyzer. Polymerization grade ethylene was supplied by Beijing Yansan Petrochemical Co. Et₂AlCl (1.90 M in toluene) and AlEt₃ (2 M in hexane) were purchased from Acros Chemicals, while methylaluminoxane (MAO, 1.46 M in toluene) and modified methylaluminoxane (MMAO, 1.93 M in heptane) were purchased from Akzo Nobel Corp. ¹³C NMR spectra of the copolymers were recorded on a Bruker DMX 300 MHz instrument at 135 °C in deuterated 1,2-dichlorobenzene with TMS as an internal standard. The GPC curves were obtained by plotting detector response versus elution volume using polystyrene standards (with an approximate polydispersity index). Further fractionalization of fractions was not performed. Melting points of polyolefins were measured on a Perkin-Elmer DSC-7 differential scanning calorimetry (DSC) analyzer. Under a nitrogen atmosphere, a sample of about 2.0–6.0 mg was heated from 50 to 160 °C at a rate of 10 °C/min and kept for 5 min at 160 °C to remove the thermal history and then cooled at a rate of 10 °C/min to 50 °C. The DSC trace and the melting points of the samples were obtained from the second scanning run.

4.2. Preparations of Ligands. **4.2.1. 2,6-Diisopropyl-N-(1-phenylethylidene)benzenamine (PhMeC=N(2,6- i -Pr₂C₆H₃), **1a**).** According to the literature,^{24,25} the Schiff base **1a** was recrystallized from its ethanol solution and isolated as yellow crystals (18.2 g, 65% yield). IR (KBr, cm⁻¹): 1645 ($\nu_{C=N}$). ¹H NMR (300 MHz, CDCl₃): δ 0.04 (d, 12H, CH₃, ³J_{HH} = 6.9 Hz), 1.14–1.30 (s, 3H, CH₃), 2.71 (sept, 2H, CH, ³J_{HH} = 6.9 Hz), 7.07–7.25 (m, 5H, Ph), 7.49–7.51 (s, 2H, aryl), 8.05–8.06 (s, 1H, aryl). ¹³C NMR (75 MHz, CDCl₃): δ 18.08 (CH₃CPh), 22.96, 23.20 (CH(CH₃)₂), 28.16 (CH(CH₃)₂), 127.09, 128.38, 130.37, 136.05 (Ph), 122.90, 123.26, 139.05, 146.68 (aryl), 164.74 (C=N).

4.2.2. (κ^1 -N-(1-Phenylvinyl)-2,6-diisopropylbenzenamido)magnesium Bromide ((CH₂)(Ph)C(2,6- i -Pr₂C₆H₃)NMgBr·2THF, **1b).** LDA (0.21 g, 2 mmol) was added to a cold solution of **1a** (0.56 g, 2 mmol) in 25 mL of THF, and the mixture was stirred for 3 h at -78 °C. To the suspension was added MgBr₂ (0.37 g, 2 mmol), and this mixture was then warmed to room temperature for 5 h. The resultant solution was concentrated in vacuo and washed with hexane to give colorless crystals of **1b** (1.03 g, 98% yield). Mp: 182–183 °C dec. ¹H NMR (300 MHz, C₆D₆): δ 1.11 (d, 12H, CH(CH₃)₂, ³J_{HH} = 6.9 Hz), 2.62 (sept, 2H, CH(CH₃)₂, ³J_{HH} = 6.6 Hz), 4.08–4.10 (d, 2H, CH₂, ³J_{HH} = 6.3 Hz), 7.23–7.30 (m, 5H, Ph), 7.38–7.41 (m, 3H, aryl). ¹³C NMR (75 MHz, C₆D₆): δ 24.44, 26.57 (CH(CH₃)₂), 31.33 (CH(CH₃)₂), 96.45 (CH₂), 126.12 (*p*-Ar), 130.29 (*m*-Ar), 131.45 (*o*-Ph), 133.76 (*p*-Ph), 134.05 (*m*-Ph), 138.66 (*ipso*-C_{Ph}), 139.12 (*ipso*-C_{Ar}), 141.77 (*ipso*-C_{Ar}-N), 168.39 (N=C). Found: C, 63.81; H, 7.68; N, 2.70. Anal. Calcd for C₃₉H₄₀MgBrNO₂: C, 63.83; H, 7.65; N, 2.66.

4.2.3. N-(2-((Dimethylamino)dimethylsilyl)-1-phenylvinyl)-2,6-diisopropylbenzenamine (Me₂NMe₂SiCH₂(Ph)CN(2,6- i -Pr₂C₆H₃), **1c).** To a solution of **1b** (1.05 g, 2 mmol) in 25 mL of THF at 0 °C, was transferred Me₂NMe₂SiCl (0.30 mL, 2 mmol) dropwise to form a rose red solution; this color gradually disappeared and changed to yellow. The mixture was then warmed to room temperature and stirred for 12 h. The resulting white residue was extracted with 50 mL of toluene, and removal of the solvent under reduced pressure gave a yellow oil of **1c** (0.75 g, 97% yield). Attempts to purify the product by extraction with hexanes were unsuccessful because of the high solubility of the yellow oil in all these solvents. ¹H NMR (300 MHz, CDCl₃): δ 0.01 (d, 6H, Si(CH₃)₂), 1.08 (s, 2H, CH₂), 1.37 (sept, 12H, CH(CH₃)₂, ³J_{HH} = 6.9 Hz), 2.33–2.48 (d, 6H, N(CH₃)₂), 2.98 (sept, 2H, CH(CH₃)₂, ³J_{HH} = 6.9 Hz), 7.22–7.30 (m, 5H, Ph), 7.59 (s, 2H, *m*-Ar), 8.03 (d, H, *p*-Ar).

4.2.4. Lithium κ^1 -N-(2-((Dimethylamino)dimethylsilyl)-1-phenylvinyl)-2,6-diisopropylbenzenamidate (Me₂NMe₂SiCH(Ph)C(2,6- i -Pr₂C₆H₃)NLi·3THF, **1d).** To a solution of **1c** (0.76 g, 2 mmol) in 25 mL of THF at -78 °C was added LDA (0.22 g, 2 mmol) to form a yellow solution; this color gradually disappeared and changed to brown. The mixture was stirred for 2 h and then warmed to room temperature and stirred for 12 h. A bright yellow solid was obtained (0.76 g, 98% yield) by concentrating the THF solution under a nitrogen atmosphere. Crystallization from hexane and THF (4:1) afforded yellow crystals of **1d** (1.17 g, 97% yield). ¹H NMR (300 MHz, C₆D₆): δ -0.10–0.10 (d, 6H, Si(CH₃)₂), 0.67–0.71 (2 sept, 12H, CH(CH₃)₂, ³J_{HH} = 5.7 Hz), 0.76–0.83 (q, 12H, 3THF), 2.25 (s, 6H, N(CH₃)₂), 2.80 (q, 12H, 3THF), 3.13 (d, H, CH, ³J_{HH} = 5.1 Hz), 3.33 (sept, 2H, CH(CH₃)₂, ³J_{HH} = 6.9 Hz), 6.44–6.49 (q, 2H, *o*-Ph), 6.53–6.61 (m, 3H, *m,p*-Ph), 6.68 (s, 1H, *p*-Ar), 7.10–7.13 (m, 2H, *m*-Ar). ¹³C NMR (75 MHz, C₆D₆): δ -3.96 (Si(CH₃)₂), 23.85–24.58 (CH₃, ⁱPr), 26.03 (CH₂, THF), 28.38–29.45 (CH, ⁱPr), 38.86 (N(CH₃)₂), 68.43 (O-CH₂, THF), 73.36 (CH), 121.34 (*p*-Ar), 123.51 (*m*-Ar), 126.57 (*o*-Ph), 127.44 (*p*-Ph), 129.37 (*m*-Ph), 143.09 (*ipso*-C_{Ph}), 146.35 (*ipso*-C_{Ar}), 152.14 (*ipso*-C_{Ar}-N), 172.90 (N=C). Found: C, 71.69; H, 9.83; N, 4.64. Anal. Calcd for C₃₆H₅₉LiN₂O₃Si: C, 71.72; H, 9.86; N, 4.65.

(24) (a) Coleman, K. S.; Green, M. L. H.; Pascu, S. I.; Rees, N. H.; Cowley, A. R.; Rees, L. H. *Dalton Trans.* **2001**, 3384. (b) Pascu, S. I.; Coleman, K. S.; Cowley, A. R.; Green, M. L. H.; Rees, N. H. *New J. Chem.* **2005**, 29, 385.

(25) Okamoto, H.; Shozo, K.; Gasawara, M.; Konnai, M.; Takematsu, T. *Agric. Biol. Chem.* **1991**, 55, 2733.

4.3. Synthesis of Compounds 2 and 3. **4.3.1. Bis(η^3 -*N*-2-((dimethylamino)dimethylsilyl)-1-phenylvinyl)-2,6-diisopropylanilido}zirconium Dichloride ($\{\eta^3$ -(2,6- $\text{Pr}_2\text{C}_6\text{H}_3$)N(Ph)CCHSiMe₂NMe₂ $\}_2\text{ZrCl}_2$, **2**). To a solution of **1d** (1.21 g, 2 mmol) in 25 mL of THF at -78°C was added ZrCl_4 (0.23 g, 1 mmol) to form a rose-colored solution, and its color gradually changed to yellow. The mixture was stirred for short time and then warmed to room temperature and stirred for 24 h. Volatile compounds were removed in vacuo, and the resulting residues were solvated in 30 mL of CH_2Cl_2 . The filtrate was concentrated and recrystallized at -20°C as colorless crystals of **2** (0.64 g, 69% yield). Mp 159 – 161°C dec. ^1H NMR (300 MHz, CDCl_3): δ 0.21 (s, 12H, Si(CH_3)₂), 0.84, 0.87, 1.03, 1.15 (4 sept, 24H, CH(CH_3)₂), $^3J_{\text{HH}} = 6.6$ Hz), 2.11 (s, 12H, N(CH_3)₂), 2.56, 2.89 (2 sept, 4H, CH(CH_3)₂), $^3J_{\text{HH}} = 6.9$ Hz), 1.49, 4.09 (d, 2H, CH, $^3J_{\text{HH}} = 6.9$ Hz), 6.91 (q, 4H, *o*-Ph), 6.99–7.05 (m, 6H, *m*, *p*-Ph), 7.14 (m, 4H, *m*-Ar), 7.33–7.45 (m, 2H, *p*-Ar). ^{13}C NMR (75 MHz, CDCl_3): δ 14.45 (Si(CH_3)₂), 22.79, 24.89, 28.79, 31.93 (CH₃, iPr), 19.19 (CH, iPr), 38.68 (N(CH_3)₂), 69.27 (CH), 123.55, 125.36, 127.97 (Ar and Ph), 131.64 (*ipso*-C_{Ph}), 137.04, 147.54 (*ipso*-C_{Ar}). Found: C, 62.60; H, 7.62; N, 6.12. Anal. Calcd for C₄₉H₇₀Cl₂N₄Si₂Zr: C, 62.57; H, 7.66; N, 6.08.**

4.3.2. $\{\eta^3$: η^1 -*N*-2-((Dimethylamino)dimethylsilyl)-1-phenylvinyl)-2,6-diisopropylanilido}zirconium Trichloride [$\{\eta^3$: η^1 -(2,6- $\text{Pr}_2\text{C}_6\text{H}_3$)N(Ph)CCHSiMe₂NMe₂ $\}_2\text{ZrCl}_3$, **3]. Using the same procedure as for **2** but with equimolar reactants of lithium and zirconium, the resultant residue was extracted with dichloromethane and the extract filtered. The filtrate was concentrated in vacuo and dissolved in a mixture of CH_2Cl_2 and THF (3:1) at -20°C to give compound **3** as yellow crystals (1.01 g, 87% yield). Mp: 167 – 169°C dec. ^1H NMR (300 MHz, C_6D_6): δ -0.02 to $+0.03$, 0.31 – 0.36 (q, 6H, Si(CH_3)₂), 0.56, 0.93, 1.29, 1.70 (4 sept, 12H, CH(CH_3)₂), $^3J_{\text{HH}} = 7.2$ Hz), 2.26 (d, 6H, N(CH_3)₂), $^3J_{\text{HH}} = 11.1$ Hz), 3.79 (sept, 2H, CH(CH_3)₂), $^3J_{\text{HH}} = 6.9$ Hz), 4.54 (s, H, CH), 6.84–6.99 (m, 5H, Ph), 7.34–7.37 (m, 3H, aryl). ^{13}C NMR (75 MHz, C_6D_6): δ -1.36 , -0.48 (Si(CH_3)₂), 21.30, 22.54, 24.21, 25.96 (CH(CH_3)₂), 35.54 (CH(CH_3)₂), 40.33, 42.95 (N(CH_3)₂), 80.88 (CH), 93.50, 121.57, 123.02, 124.17, 129.79 (aryl and Ph), 132.50 (*ipso*-C_{Ph}), 134.35, 138.00, 140.90 (*ipso*-C_{Ar}), 173.84 (NCC). Found: C, 49.91; H, 6.09; N, 4.83. Anal. Calcd for C₂₄H₃₅Cl₃N₂SiZr: C, 49.94; H, 6.11; N, 4.85.**

4.4. Procedures for Ethylene Polymerization. **4.4.1. Polymerization under 1 atm of Ethylene.** The compound ($5\ \mu\text{mol}$) was added to a Schlenk type flask under nitrogen. This flask was back-filled three times with nitrogen and twice with ethylene and then charged with the required amount of freshly distilled toluene. At the stipulated temperature the reaction solution was vigorously stirred under 1 atm of ethylene for the desired period of time, after which the MAO solution was added to start

the polymerization. The polymerization reaction was quenched by adding 10% HCl–ethanol solution (60 mL), and then the mixture was poured into 100 mL of ethanol to precipitate the polymer, which was further washed with ethanol and water followed by drying under vacuum at 60°C to its constant weight. In the case of ethylene/1-hexene copolymerization, 1-hexene (dried with calcium hydride) solution in toluene was added prior to the addition of MAO.

4.4.2. Polymerization under 10 atm of Ethylene. For polymerization at higher ethylene pressure, a stainless steel autoclave (0.5 L capacity) equipped with gas ballast through a solenoid valve for continuous feeding of ethylene at constant pressure was used. The autoclave was heated under vacuum to over 80°C , recharged with ethylene three times, and then cooled to room temperature. A toluene solution of the catalysts (and monomer) was transferred to the reactor, which was then maintained at the desired temperature. MAO solution to give a final volume of 100 mL was then added to start the polymerization; then the autoclave was immediately pressurized to the desired pressure. At the end of the reaction time the polymerization reaction was stopped and the autoclave was placed in a water–ice bath for 1 h when 10% HCl–acidic ethanol was added. The solid polyolefin was washed with ethanol and water several times and then dried under vacuum to constant weight.

4.5. X-ray Crystallography. Data collection of **1b,d**, **2**, and **3** was performed with Mo $K\alpha$ radiation ($\lambda = 0.71073\ \text{\AA}$) on a Bruker Smart Apex CCD diffractometer at 223(2) K. Crystals were coated in oil and then directly mounted on the diffractometer under a stream of cold nitrogen gas. A total of N reflections were collected by using ω scan mode. Intensities were corrected for Lorentz and polarization effects and empirical absorption. The structures were solved by direct methods and refined by full-matrix least-squares on F^2 . All non-hydrogen atoms were refined anisotropically. The hydrogen atoms were placed in calculated positions. Structure solution and refinement were performed by using the SHELXL-97 package.²⁶ Crystal data collection and refinement details for all compounds are available in the Supporting Information.

Acknowledgment. We thank the Natural Science Foundation of China (Nos. 20772074 and 20702029).

Supporting Information Available: Figures giving ^{13}C NMR spectra for poly(ethylene-co-1-hexene) and a table and CIF files giving crystal data and processing parameters and crystallographic data for compounds **1b,d**, **2**, and **3**. This material is available free of charge via the Internet at <http://pubs.acs.org>.

(26) Sheldrick, G. M. *Program for the Solution of Crystal Structures*; University of Göttingen: Göttingen, Germany, 1997.